

# Boltzmann convolutions and Welford mean-variance layers with an application to time series forecasting and classification

Daniel Andrew Coulson<sup>1</sup> and Martin T. Wells<sup>2</sup>

<sup>1,2</sup>Department of Statistics and Data Science, Cornell University, Ithaca, NY 14853

## Abstract

In this paper we propose a novel problem called the ForeClassing problem where the loss of a classification decision is only observed at a future time point after the classification decision has to be made. To solve this problem, we propose an approximately Bayesian deep neural network architecture called ForeClassNet for time series forecasting and classification. This network architecture forces the network to consider possible future realizations of the time series, by forecasting future time points and their likelihood of occurring, before making its final classification decision. To facilitate this, we introduce two novel neural network layers, Welford mean-variance layers and Boltzmann convolutional layers. Welford mean-variance layers allow networks to iteratively update their estimates of the mean and variance for the forecasted time points for each inputted time series to the network through successive forward passes, which the model can then consider in combination with a learned representation of the observed realizations of the time series for its classification decision. Boltzmann convolutional layers are linear combinations of approximately Bayesian convolutional layers with different filter lengths, allowing the model to learn multitemporal resolution representations of the input time

series, and which resolutions to focus on within a given Boltzmann convolutional layer through a Boltzmann distribution. Both layers are novel additions to the deep learning practitioners' tool kit, which would be helpful in problems concerned with using neural networks to make decisions with sequential data regarding future events. Through several simulation scenarios and two real world applications we demonstrate ForeClassNet achieves superior performance compared with current state of the art methods including a near 30% improvement in test set accuracy in our financial example compared to the second best performing model.

**Keywords:** Bayesian deep learning, convolutional networks, classification, ECG classification, forecasting, multi-task learning, stock price prediction, time series

Notebooks containing the results discussed and the code to produce those results can be found at: <https://danielcoulson.github.io/research/>.

## 1 Introduction

Decision makers face daily instances of making decisions in temporal scenarios; for example, as a stock trader, should I buy or sell a stock based on the previous and expected future prices; or as a doctor, based on past ECG observations, with which heart condition should I diagnose a patient? These decisions involve a sequence of past observations and a classification decision to be made, where the rewards and consequences of that decision are only observed after you have made the decision.

The area of study that attempts to address such problems is Time Series Classification (TSC). Specifically, given an observed time series, to which class should I assign this time series? For example, for the stock trader, given the past history of a stock, what position should they take? There is a rich and growing literature on time series classification over the past decade, with review articles such as Middlehurst et al. [2024b], Mohammadi Foumani et al. [2024], and Ruiz et al. [2021] highlighting the most significant developments in the literature. Despite this, there is minimal literature on the real-world scenario in which we wish to make a classification decision based on ob-

served and unobserved (future) realizations of a time series. Naturally, as humans our initial thoughts are what is likely to happen next, and based upon how likely we believe various scenarios to transpire, we will then make a classification decision regarding the action to take. For example, as a stock trader (Section 5.2) I would first consider the events that I believe could happen. Based on this, I would forecast future prices of the stock and a measure of how likely I think each of these prices will occur. Finally, based upon the previous prices, my predictions of the future prices and the likelihood of them occurring, I would then decide on the position to take in the stock.

In this work, we propose a solution to this problem utilizing a single approximately Bayesian neural network, which first forecasts a time series. Through the Welford mean-variance layer, the network then iteratively updates its estimates of the mean and variance for each forecasted time point by means of successive forward passes through the network. After this, the model then makes a classification decision based on the forecast means and variances in combination with a learned abstract representation of the observed time series, where the learned representation is with respect to the forecasting problem rather than the classification problem.

We will compare our method to the two state-of-the-art methods highlighted in Middlehurst et al. [2024b], HIVE-COTE 2 (Middlehurst et al. [2021]) and Multi-Rocket Hydra (Dempster et al. [2023]). HIVE-COTE 2 (Hierarchical Vote Collection of Transformation-based Ensembles) is an ensemble of several time series classifiers; with different classifiers corresponding to different representations of time series used in the TSC literature, for example dictionary-based or distance-based representations. Although this, however, achieves state-of-the-art accuracy on many problems, it struggles to cope with large problems. To alleviate this, the authors introduce a user-specified time contract where now the different components of HIVE-COTE 2 (HC2) build as many classifiers as they can within the given time frame. However, we still found that in some of our experiments the current implementation of HC2 in the `aeon` package (Middlehurst et al. [2024a]) can exceed the time contract. Multi-Rocket Hydra (MR-Hydra)

is a mixture of a convolutional approach and a dictionary-based approach. MR-Hydra relies on random convolutional filters along with other operations to transform the time series. The convolutional approach is then combined with the dictionary approach, with the kernels being placed into groups, and the number of times each kernel within a given group has the largest activation is counted.

Some other related techniques in the literature are early classification methods, which aim to classify a time series as soon as possible, that is, using as few observed time points as required. We will be using the TEASER method (Schäfer and Leser [2020]) as a further comparison means for our method. TEASER uses a two-tier classification system. In the first tier, a classifier outputs class probabilities for the given classes a time series could be in, with these probabilities then being passed to a subsequent classifier to determine if the probabilities are sufficiently large for a reasonable classification decision to be made. The early classification problem is different from the problem we have discussed in that we are interested in future classification based on what has happened and what we think will happen. Deep learning approaches are usually not as successful as other approaches used in the TSC literature. The best deep network for time series classification (Ismail Fawaz et al. [2020]) is a network consisting of inception-modules based upon the work of Szegedy et al. [2015] in the computer vision literature and utilize multiple convolutional filters of different lengths.

However, none of these methods have built-in machinery for time-series forecasting, which inhibits their performance when the class to which a time series belongs is a function of both the observed and future realizations of the time series.

Some works in the literature are related to the problem discussed in this paper, for example Alonso et al. [2006], Vilar and Vilar [2013], and Lee et al. [2014]. They utilize forecast densities to perform unsupervised time series clustering of the forecasts of different time series. These methods are not applicable to the current work because we deal with supervised rather than unsupervised learning, particularly classification instead of clustering. Liu et al. [2014] extends the use of forecast densities for time

series clustering to both the unsupervised and supervised setting. However, in their paper they assume the time series follow autoregressive processes of order  $p$ . However, a fixed autoregressive structure of order  $p$ , limits the variety of time series dynamics that can be modeled, thus reducing the applicability of this approach especially in modern data sets where we often see realizations from what appear to be more exotic stochastic processes. Furthermore, the method relies on using a nonparametric bootstrap procedure to obtain estimates of forecast densities. This in combination with the specified AR form has the problem of leading to possibly a larger generalization error. This method also requires that, once the forecast densities have been obtained, a polarization measure for each pair of time series must be computed, which becomes prohibitive for modern data sets. Other related works in the literature include Fröhwrth-Schnatter and Kaufmann [2008] and Gür et al. [2015] which cluster time series into groups that share the same model and then perform some form of forecasting using all observations within a given group.

The aim of this present work is to have a single model that can simultaneously perform time series forecasting and classification. Desiring flexibility and to minimize the amount of input required on the user end, we avoid the traditional Box-Jenkins approach to model building and the ARIMA family of models, which are often used to model a specific time series rather than being used to model many time series simultaneously, which is the domain of more flexible models like artificial neural networks (ANNs) as utilized in this paper.

Future observations of a time series have associated uncertainty as to the possible outcome, thus we want our model to have some measure of the uncertainty associated with its own forecasts of the future. Therefore, we employ an approximately Bayesian neural network, using Monte Carlo dropout (Gal and Ghahramani [2016]). In their paper the authors consider a single hidden layer neural network where dropout is applied during both training and testing. They show that the objective function of such a model is approximately equivalent to a Gaussian process. By stacking multiple lay-

ers in a network, this is approximately equivalent to that of a deep Gaussian process (Damianou and Lawrence [2013]). Furthermore, by using Monte Carlo dropout, this allows for easy incorporation of our proposed model and neural network layers into existing deep learning pipelines, as this simply requires the application of dropout at both training and inference time. However, standard Monte Carlo dropout requires tuning of the dropout probabilities, which can be computationally expensive. To avoid this Gal et al. [2017] apply a concrete relaxation to allow learning of the dropout probabilities which we will utilize in this present work. To incorporate the uncertainty of our model forecasts into the proceeding classification output of the model, we propose a novel layer for computing the mean and variance of the model forecasts, which we call a Welford mean-variance layer. For each time series under consideration, we iteratively update the estimates of its means and variances for each of its forecasted time points by means of successive forward passes through the network, where we utilize Welford’s algorithm (Welford [1962]) for the online computation.

In TSC there are certain patterns, for example, increasing and decreasing periods, or peaks and troughs, which as humans we would often look at if we were solving the TSC problem; these should be hard coded into models to ensure they capture these shapes and to allow the other learnable components to focus on less obvious and abstract representations of an observed time series. To do this, we use hand-made filters, based on the work of Ismail-Fawaz et al. [2022], in the first layer of our network with a parallel learnable layer, which are then subsequently combined in a concatenation layer. However, these are hand-crafted filters and therefore nonprobabilistic. From the viewpoint of having a Bayesian network, this is undesirable. Therefore, we propose Boltzmann convolutional layers (BCs) as an alternative to standard convolutional layers. We construct a set consisting of several possible filter lengths prior to training our network and allow these filter lengths to follow a Boltzmann distribution, where the "energies" of the different convolutional filter lengths are learned during training, and the output of a BC layer is a linear combination of the outputs of convolutional layers

with a given filter length, weighted by the learned probabilities associated with each filter length. This also allows our model to be able to represent a variety of dynamics and learn from the data which filter lengths to focus on as a form of model selection, rather than having a single filter length, which is often crudely chosen. We also use BC layers with learnable filters in our network to provide additional flexibility.

BC layers relate to some of the existing literature on neural architecture search. For example, Chen et al. [2020] discusses dynamic convolutions (DC). However, DC uses linear combination weights that vary for each input time series, whereas our BC layers have the same weights for each input time series. This dynamic approach makes sense for certain applications, but for the applications we consider, we are trying to learn a representation of time series, which will allow us to discriminate between one of several possible stochastic processes. Having dynamic weights stymies this goal, which detracts from interpretability where the model will be looking at different aspects of each input time series despite them being time series associated with the same problem, where as BC layers allow for more homogeneous learning of the generating stochastic process(es). Furthermore, the linear combination weights are calculated using a squeeze and excitation approach (Hu et al. [2018]). Instead, BC layers have a simpler approach of training the energies within a Boltzmann distribution to compute the linear combination weights; which also provides some flexibility to users on which resolutions they want the model to focus on within a given BC layer through variation of the temperature parameter, which we discuss further in Section 2.1. Moreover, DC have the same filter length for each convolutional kernel, whereas we are interested in a multi-temporal resolution representation of our time series to aid the discriminative ability of our network. Finally, DC only has linear combinations of convolutional kernels, whereas BC layers have linear combinations of convolutional layers. This allows our model to perform a form of soft model selection within each BC layer, allowing the model to choose which temporal resolutions to focus on while maintaining a multi-temporal resolution representation through the linear combination of the convolutional layers. Although

this could be more computationally expensive, each convolutional layer within a BC layer is wrapped in a spatial Monte Carlo dropout module, which reduces the number of active convolutional kernels within a BC layer for a given forward and backward pass through the network. This also allows for approximate Bayesian inference and subsequent uncertainty quantification which can be exploited within the network. The work of Wang et al. [2021] builds on DC by now allowing different filter lengths within the convolutional kernels that make up the DC kernel, but it still suffers from the other problems of DC mentioned above when compared to BC layers.

Both the BC and Welford mean-variance layers can be used in existing ANN architectures and prove promising additions to the deep learning toolkit. BC layers allow for flexible model selection and multiresolution representations. Welford mean-variance layers allow for the computation of means and variances within stochastic neural networks, which can then be used by neural networks to represent uncertainty about unknown information and be passed on to subsequent layers within the network. This paper will proceed as follows. In Section 2 we define our motivating problem, which we call the ForeClassing problem and prove a motivating theorem, BC layers, and Welford mean-variance layers. Section 3 will discuss our network architecture for the time series ForeClassing problem which will incorporate the layers of Section 2 and a discussion on our approach to classification using the learned abstract representations for forecasting. Section 4 presents our simulation results. Section 5 presents two real-world examples, and finally Section 6 concludes and discusses suggestions for future research.

## **2 Boltzmann convolutions, Welford mean-variance layers, and the motivating problem**

In this section we discuss the two novel artificial neural network (ANN) layers we are proposing, which we use in our network for time series classification (see Section 3). Firstly, we formally define the problem statement we have designed our network to



solve which was motivation for Boltzmann Convolutions and Welford mean-variance layers.

**Definition 1.** *Suppose that we have  $N$  observed time series each of length  $m$ ,  $\mathbf{x}^{(i)} = (x_1^{(i)}, \dots, x_m^{(i)})^T$  for  $i = 1, \dots, N$ . Each time series is a member of one of  $L$  classes, where the class in which a time series is in is realized only in the future, say  $k$  time points ahead. We will denote the future observations of the time series by  $\mathbf{x}_*^{(i)} = (x_{m+1}^{(i)}, \dots, x_{m+k}^{(i)})^T$  and the class time series  $i$  is by  $y^{(i)} \in \{0, 1, \dots, L - 1\}$ , for  $i = 1, \dots, N$ . Where  $y^{(i)} = f(\mathbf{x}^{(i)}, \mathbf{x}_*^{(i)}) = f(\mathbf{x}^{(i)}, w(\mathbf{x}^{(i)}, \epsilon_{m+1}, \epsilon_{m+2}, \dots, \epsilon_{m+k}))$ , the function  $w$  is a mapping from the observed time series to the future observations of the time series,  $\epsilon_{m+1}, \dots, \epsilon_k$  represents the randomness associated with future outcomes which are unobserved, and  $f$  is a mapping from the observed and future time series to the class a given time series belongs. We wish to find functions which estimate  $f$  and  $w$  that minimize the loss between the true and estimated classification label and the predicted forecast value, respectively, for each time series.*

Note in Definition 1 to compute the class label of the time series, we need to know  $\mathbf{x}_*^{(i)}$ , however, this is unknown at the present time point, so we need to find a further function  $w$  which forecasts the future time points of the series. This can be thought somewhat analogously to hand-crafted filters in that we are providing more direction as to what functions the model should learn, particularly those helpful in forecasting. To facilitate a model incorporating uncertainty into its classification decision, we propose Welford mean-variance layers for use in Bayesian networks. In this paper, we use an approximately Bayesian neural network to quantify uncertainty. We also have pre-defined hand-crafted filters that are nonrandom. To allow all components of the network to be random, we propose Boltzmann convolutions.

In Bayesian inference, we have observed data  $\mathbf{x}$  and a model of these data (assuming the densities exist) with probability density function  $p(\mathbf{x}|\boldsymbol{\theta})$ , where  $\boldsymbol{\theta}$  is an unknown parameter vector and the goal is to find the distribution of the parameters conditional on the observed data with probability density function  $p(\boldsymbol{\theta}|\mathbf{x})$  known as the posterior

distribution. By Bayes theorem we have that

$$p(\boldsymbol{\theta}|\mathbf{x}) = \frac{p(\mathbf{x}|\boldsymbol{\theta})p(\boldsymbol{\theta})}{p(\mathbf{x})}, \text{ where } p(\mathbf{x}) = \int_{\boldsymbol{\theta}} p(\mathbf{x}|\boldsymbol{\theta})p(\boldsymbol{\theta})d\boldsymbol{\theta},$$

where  $p(\boldsymbol{\theta})$  is known as the prior distribution and represents ones beliefs about  $\boldsymbol{\theta}$  before observing any data. The usual method to conduct Bayesian inference is using Markov Chain Monte Carlo(MCMC) due to asymptotic guarantees through the Markov Chain approach where one creates a Markov Chain whose stationary distribution is the posterior distribution of interest. However, MCMC can be computationally expensive and inference infeasible when one has a large number of parameters and many chains. Variational inference(VI) provides an alternative and faster path by framing Bayesian inference as an optimization procedure in terms of minimizing the Kullback-Leibler (KL) divergence between the target posterior distribution and a simplified distribution we are trying to optimize for, however the speed of VI is at the cost of the asymptotic guarantees. Due to the large number of parameters in a neural network MCMC is not practical instead practitioners opt for VI instead. That is we wish to find  $\arg \min_{f(\boldsymbol{\theta}) \in D} KL(f(\boldsymbol{\theta})||p(\boldsymbol{\theta}|\mathbf{x}))$ , where  $D$  is a class of probability distributions often assumed to follow the mean-field assumption containing the candidate variational distributions. However, the KL divergence is often computationally intractable so instead VI maximizes a quantity called the evidence lower bound (ELBO) which is equivalent to minimizing  $KL(f(\boldsymbol{\theta})||p(\boldsymbol{\theta}|\mathbf{x}))$ . Particularly,

$$ELBO(f(\boldsymbol{\theta})) = \mathbb{E}_{f(\boldsymbol{\theta})}[log(p(\boldsymbol{\theta}, \mathbf{x})) - log(f(\boldsymbol{\theta}))].$$

To perform Bayesian inference in our network we use Monte Carlo dropout proposed by Gal and Ghahramani [2016] where the authors show that minimizing the objective of a dropout neural network also approximately minimizes the KL divergence between the variational distribution and the posterior distribution of a deep Gaussian process(Damianou and Lawrence [2013]). For Bayesian inference in this work we use

concrete dropout proposed in Gal et al. [2017] which builds upon Monte Carlo dropout by allowing the automatic tuning of the dropout probabilities.

Definition 1 and the following theorem, the ForeClassing Theorem, highlight the need for models that solve the ForeClassing Problem rather than only the classification problem.

**Theorem 1.** *Consider the probability space  $(\Omega, \mathcal{F}, \mathbb{P})$  and the random variables  $\mathbf{X} : \Omega \rightarrow \mathbb{R}^m$ ,  $\mathbf{X}_* : \Omega \rightarrow \mathbb{R}^k$ , and  $Y : \Omega \rightarrow \{0, 1\}$ , where  $Y = f(\mathbf{X}, \mathbf{X}_*)$  for some unknown measurable function  $f(\cdot)$ . Assume  $\mathbf{X}_*$  is not fully determined by  $\mathbf{X}$ , that is,  $\sigma(\mathbf{X}) \subsetneq \sigma(\mathbf{X}, \mathbf{X}_*)$ . In addition, assume that  $\mathbf{X}_*$  provides additional information regarding  $Y$  beyond  $\mathbf{X}$  i.e.  $\exists A \in \sigma(\mathbf{X}_*) \setminus \sigma(\mathbf{X})$  where  $\mathbb{P}(A) > 0$  such that  $\mathbb{P}(Y = y | \mathbf{X}, \mathbf{X}_*) \neq \mathbb{P}(Y = y | \mathbf{X})$ . Then for any classifier  $\tilde{f}(\mathbf{X})$  that ignores  $\mathbf{X}_*$  there exists a classifier  $\hat{f}(\mathbf{X}, \mathbf{X}_*)$  whose classification error is strictly smaller.*

*Proof.* Consider the two Bayes optimal classifiers,

$$\tilde{f}_{\text{Bayes}}(\mathbf{X}) = \arg \max_{y \in \{0,1\}} \mathbb{P}(Y = y | \mathbf{X} = \mathbf{x})$$

and

$$\hat{f}_{\text{Bayes}}(\mathbf{X}, \mathbf{X}_*) = \arg \max_{y \in \{0,1\}} \mathbb{P}(Y = y | \mathbf{X} = \mathbf{x}, \mathbf{X}_* = \mathbf{x}_*).$$

Their respective expected risks under the 0-1 loss are given by

$$R(\tilde{f}_{\text{Bayes}}(\mathbf{X})) = \mathbb{E}_{\mathbf{x} \sim \mu_{\mathbf{X}}} [1 - \max_{y \in \{0,1\}} \mathbb{P}(Y = y | \mathbf{X} = \mathbf{x})]$$

and

$$R(\hat{f}_{\text{Bayes}}(\mathbf{X}, \mathbf{X}_*)) = \mathbb{E}_{(\mathbf{x}, \mathbf{x}_*) \sim \mu_{\mathbf{X} \times \mathbf{X}_*}} [1 - \max_{y \in \{0,1\}} \mathbb{P}(Y = y | \mathbf{X} = \mathbf{x}, \mathbf{X}_* = \mathbf{x}_*)].$$

Since  $\mathbf{X}_*$  contains additional information about  $Y$  beyond  $\mathbf{X}$ , we have

$$\max_{y \in \{0,1\}} \mathbb{P}(Y = y | \mathbf{X} = \mathbf{x}, \mathbf{X}_* = \mathbf{x}_*) > \max_{y \in \{0,1\}} \mathbb{P}(Y = y | \mathbf{X} = \mathbf{x}).$$

This implies that

$$1 - \max_{y \in \{0,1\}} \mathbb{P}(Y = y | \mathbf{X} = \mathbf{x}, \mathbf{X}_* = \mathbf{x}_*) < 1 - \max_{y \in \{0,1\}} \mathbb{P}(Y = y | \mathbf{X} = \mathbf{x}).$$

Taking expectations, we obtain

$$\mathbb{E}_{(\mathbf{x}, \mathbf{x}_*) \sim \mu_{\mathbf{X}} \times \mu_{\mathbf{X}_*}} [1 - \max_{y \in \{0,1\}} \mathbb{P}(Y = y | \mathbf{X} = \mathbf{x}, \mathbf{X}_* = \mathbf{x}_*)] < \mathbb{E}_{\mathbf{x} \sim \mu_{\mathbf{X}}} [1 - \max_{y \in \{0,1\}} \mathbb{P}(Y = y | \mathbf{X} = \mathbf{x})].$$

Thus, we can then conclude that

$$R(\hat{f}_{Bayes}(\mathbf{X}, \mathbf{X}_*)) < R(\tilde{f}_{Bayes}(\mathbf{X})) \leq R(\tilde{f}(\mathbf{X})),$$

where  $\tilde{f}(\mathbf{X})$  is any classifier that ignores  $\mathbf{X}_*$ . □

## 2.1 Boltzmann convolutional layers

In this subsection we propose Boltzmann convolutional layers (BC), which are linear combinations of convolutional layers that are weighted by the probabilities associated with each filter length according to a Boltzmann distribution.

Firstly, we define in advance the filter lengths we are interested in, for example, suppose that we are interested in including the following filter lengths  $z := \{3, 6, 12, 18, 24, 30, 36\}$ . Then we would initialize the convolutional layers  $|z|$ , where  $|z|$  denotes the cardinality of the set  $z$ , where in the current example  $|z| = 7$ . We then allow the filter lengths to follow a Boltzmann distribution where,

$$\mathbb{P}(\text{kernel filter length} = z_j) = \text{softmax}\left(\frac{1}{T}\mathbf{p}\right)_j = \frac{\exp\{\frac{p_j}{T}\}}{\sum_{i=1}^{|z|} \exp\{\frac{p_i}{T}\}}. \quad (1)$$

In (1)  $T$  is the temperature of the distribution and  $\mathbf{p}$  is the vector of energies for the filter lengths (the set  $z$ ). In our approach, we set  $T = 1$  (a standard softmax function); however, users can also set their own temperature values if they want to

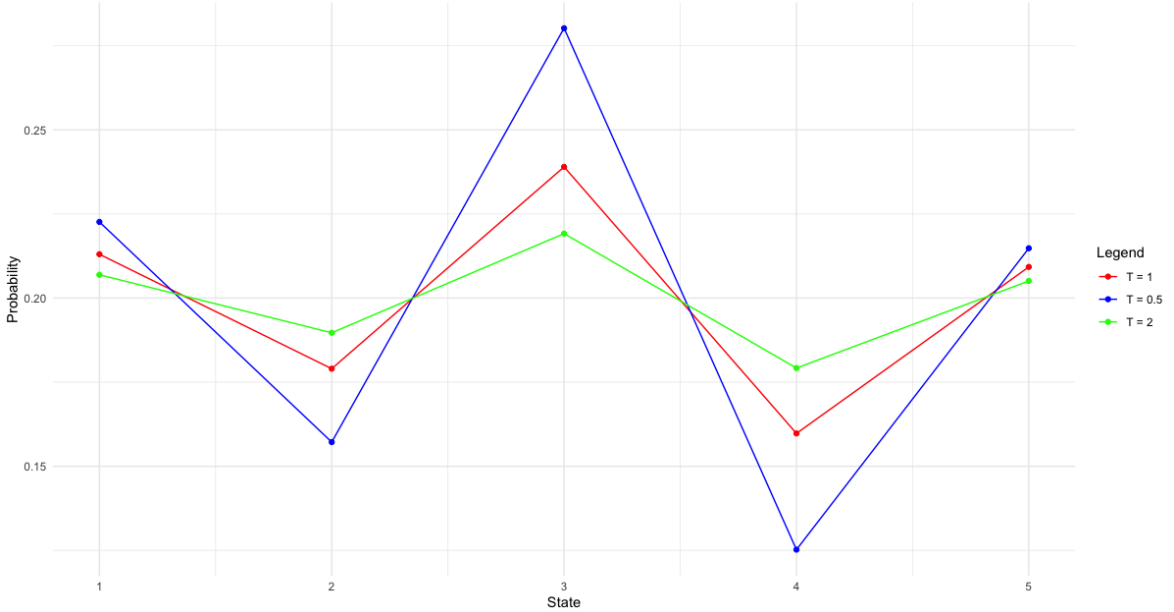


Figure 1: Plot of the Boltzmann distribution with 5 states for different values of temperature.

prioritize certain filter lengths or set the temperature as a learnable parameter (see Figure 1 for the impact of varying temperature on a Boltzmann distribution with five different states). We set  $T = 1$  and exclude the Boltzmann constant by absorbing it into the vector of energies. The vector of energies ( $\mathbf{p}$ ) is trainable and determines the probabilities associated with each filter length according to (1). Then the output of a BC layer with an input  $x$  is given by

$$\text{BC}(x) = \sum_{j=1}^{|z|} \mathbb{P}(\text{filter length} = z_j) [\text{convolutional layer with filter lengths equal to } z_j](x). \quad (2)$$

Furthermore, in each of the convolutional layers within a BC layer, we use causal padding to preserve temporal information (van den Oord et al. [2016]) and dilation in order to maintain the receptive field of our network. The output of the first convolutional layer with length filters  $K_1$  is then given by

$$W_h^1 * x(i) = \sum_{j=0}^{K_1-1} W_h^1(j) x(i - dj). \quad (3)$$

The dilation factor is given by  $d$ ,  $W_h$  represents the convolutional filter  $h$  in the layer, and  $x(i)$  represents an observation at the index  $i$  of a discrete time series input. For subsequent layers, say layer  $l$ , the output is given by,

$$W_h^l * f^{l-1}(i) = \sum_{j=0}^{K_l-1} \sum_{m=1}^{M_{l-1}} W_h^l(j, m) f^{l-1}(i - d_l j), \quad (4)$$

where  $f_{l-1}$  is the output of layer  $l-1$ ,  $H = 1, 2, \dots$ , |number of filters in  $l$ th layer|,  $K_l$  is the length of the filters in the  $l$ th layer,  $M_{l-1}$  is the number of filters in the previous layer, and  $d_l$  is the dilation factor in the  $l$ th layer (Borovykh et al. [2017]).

The BC layer improves upon standard convolutional layers by allowing the kernel sizes to be adaptive and based on the data. This allows the network to model different temporal dynamics and learn which temporal dynamics to prioritize. As well as time series applications BC layers could be helpful to other sequential modeling tasks such as natural language processing due to its multi-resolution representation and model selection capabilities. Each convolutional layer within a BC layer is wrapped in a spatial Concrete dropout layer (excluding the hand-crafted BC layer) which helps to prevent over fitting and means only a subset of the convolutional filter weights are updated during a single training pass through the network.

### **Example of convolutions with causal padding and a dilation rate of one**

Suppose in the first layer of a network we have a hand crafted filter layer based upon (8)-(10) in Section 3.2, with filters of length 3 and an input time series  $x(1), x(2), x(3), x(4), x(5), x(6)$ . Then we have 3 filters given by,

$$W_1^1 = [-1, 1, -1], W_2^1 = [1, -1, 1], \text{ and } W_3^1 = [-1, 2, -1]. \quad (5)$$

Then for  $1 \leq h \leq 3$  we have  $W_h^1 * x(i) = \sum_{j=0}^2 W_h^1(j)x(i-j)$ . This gives the following discrete convolutions:

$$\begin{aligned}
W_1^1 * x(1) &= -x_1, & W_2^1 * x(1) &= x_1, & W_3^1 * x(1) &= -x_1, \\
W_1^1 * x(2) &= x_1 - x_2, & W_2^1 * x(2) &= x_2 - x_1, & W_3^1 * x(2) &= -x_2 + 2x_1, \\
W_1^1 * x(3) &= -x_3 + x_2 - x_1, & W_2^1 * x(3) &= x_3 - x_2 + x_1, & W_3^1 * x(3) &= -x_3 + 2x_2 - x_1, \\
W_1^1 * x(4) &= -x_4 + x_3 - x_2, & W_2^1 * x(4) &= x_4 - x_3 + x_2, & W_3^1 * x(4) &= -x_4 + 2x_3 - x_2, \\
W_1^1 * x(5) &= -x_5 + x_4 - x_3, & W_2^1 * x(5) &= x_5 - x_4 + x_3, & W_3^1 * x(5) &= -x_5 + 2x_4 - x_3, \\
W_1^1 * x(6) &= -x_6 + x_5 - x_4, & W_2^1 * x(6) &= x_6 - x_5 + x_4, & W_3^1 * x(6) &= -x_6 + 2x_5 - x_4.
\end{aligned}$$

## 2.2 Welford mean-variance layers

In our model we are interested in classification, where the cost of the classification decision is observed at a future time point. Therefore, just as humans do when making decisions about the future, our model first forecasts the time series, then based on what the model has observed and what it thinks will happen next, it makes its classification decision. However, as humans we would consider the probability of our forecasts, that is how likely it is that what we think will happen will actually come to fruition. Therefore, we propose a novel layer to iteratively estimate the mean and variance of our forecasts in our approximately Bayesian network through each successive forward pass, which are then concatenated with the learned abstract representation of the observed time series, which we set to have a variance of zero, since it is observed.

Through each forward pass of our network, we record the predicted values of each forecasted time point for each time series. Then, according to Welford's algorithm (Welford [1962]) we update the mean and variance of each forecasted time point for each inputted time series, which are then passed on to the classification component of our model. The online updates for mean and variance according Welford's algorithm

are given by:

$$\bar{x}_n = \bar{x}_{n-1} + \frac{x_n - \bar{x}_{n-1}}{n} \text{ and } s_n^2 = \left(1 - \frac{1}{n}\right)s_{n-1}^2 + \frac{(x_n - \bar{x}_{n-1})(x_n - \bar{x}_n)}{n}, \quad (6)$$

where  $x_n$  is the observation of the variable of interest at iteration  $n$ ,  $\bar{x}_n$  is the sample mean of the variable of interest at iteration  $n$ , and  $s_n^2$  is the sample variance of the variable of interest at time  $n$ . Note that we work with the formula for the population variance rather than the sample variance which are exactly the same except the sample variance has a division by  $n - 1$  which causes initialization problems. That is, by applying Welford’s algorithm in our network using a Welford mean-variance layer, for a single time series the output of the concatenation of the learned abstract representation of the observed time series, with the output of the Welford layer is given by

$$\begin{bmatrix} \phi_1 & \phi_2 & \dots & \phi_m & \bar{\phi}_{m+1} & \dots & \bar{\phi}_{m+k} \\ 0 & 0 & \dots & 0 & \hat{v}ar(\phi_{m+1}) & \dots & \hat{v}ar(\phi_{m+k}) \end{bmatrix}^T,$$

where  $\phi_1, \dots, \phi_m$  are the learned representations of the observed time series,  $m$  is the number of observations, and the variance of each associated time point is set to zero. Subsequently,  $\bar{\phi}_{m+1}, \dots, \bar{\phi}_{m+k}$  denotes the mean predicted sample value for each predicted time point over a forecast horizon of length  $k$ , and  $\hat{v}ar(\phi_{m+1}), \dots, \hat{v}ar(\phi_{m+k})$  denotes the sample variance of the predicted values for each forecasted time point.

### 3 Problem statement and model

In this section we present our proposed network for time series forecasting and classification that incorporates our Boltzmann Convolutional (BC) layer and Welford mean-variance layer.



### 3.1 Motivation of network and loss function.

The network we have constructed is designed to solve the ForeCassing problem, which is stated in Definition 1 in Section 2. Definition 1 is motivated by the various temporal decisions humans make in their daily lives, where the cost of this decision is only realized at a future time index. As humans we would think about what will happen next and the uncertainty we have about our beliefs as to whether these events will happen, then based on the various scenarios we have formulated and the respective uncertainty we have about whether they will come to pass, we would then make our decision.

For example (Section 5.2) suppose that a stock trader wants to decide the position to take in a company’s stock before the release of its quarterly earnings, so they could take advantage of the stock price increase or decrease after the earnings are released. The stock trader would look at historical information about the stock and, based on this information, would have some ideas about what the earnings report will look like and the possibilities and probabilities of various movements of the price of the stock. Based on these possibilities and probabilities, they would then decide whether it is worth the risk and take some position in the stock.

The loss function in our work is given by

$$\begin{aligned} \text{Loss}(y^{(i)}, \hat{y}^{(i)}, \mathbf{x}_*^{(i)}, \hat{\mathbf{x}}_*^{(i)}) &= \alpha \text{categorical cross entropy}(y^{(i)}, \hat{y}^{(i)}) + \beta \text{MSE}(\mathbf{x}_*^{(i)}, \hat{\mathbf{x}}_*^{(i)}) \\ &= \beta \frac{1}{k} \sum_{j=1}^k \left( \mathbf{x}_{*,j}^{(i)} - \hat{\mathbf{x}}_{*,j}^{(i)} \right)^2 - \alpha \sum_{j=1}^L y_j^{(i)} \log(\hat{y}_j^{(i)}), \end{aligned} \quad (7)$$

where  $y^{(i)}$  is the one-hot encoded vector of the true class for example  $i$ ,  $\hat{y}^{(i)}$  is a vector containing the predicted probabilities of the  $L$  classes for example  $i$ , and  $\alpha$  and  $\beta$  are the weights for each loss function. In this work, we set  $\alpha = \beta = 1$ . In addition, the regularization terms for the weights in each concrete dropout layer and the dropout probabilities are also added to the loss function (7).

### 3.2 Network architecture: ForeClassNet

In this Section we first provide a representation of our network (Figure 2) which we call ForeClassNet and then discuss each component in turn. For training our network, we

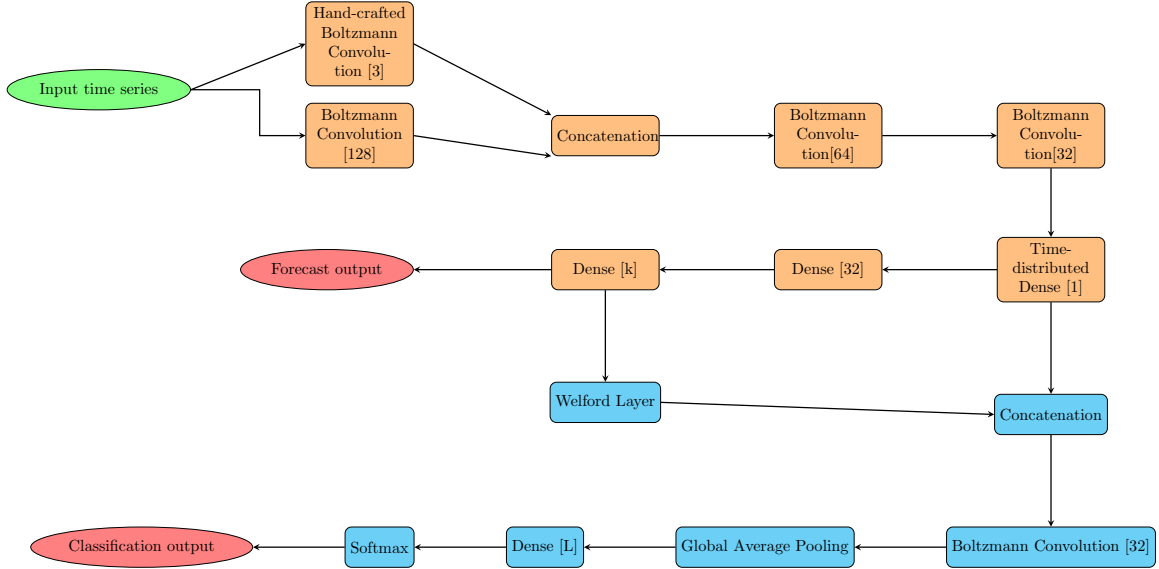


Figure 2: Graphic of our proposed network for time series forecasting and classification. The numbers in the brackets represents how many nodes are in a given layer for example Dense  $[k]$  represents a dense layer with  $k$  nodes.

have  $N$  input time series of length  $m$ , the corresponding forecast output for each of the  $m$  time series of length  $k$ , and the one-hot-encoded classification labels for each of the  $m$  time series. The input is first fed through a block consisting of two BC layers with a concatenation layer at the end. For the hand-crafted filters we build upon the work of Ismail-Fawaz et al. [2022] using an increasing and decreasing filter, and a peak filter derived from Pascal’s triangle instead of the normal probability density function, and

adapting the filters to causal, rather than forward looking convolutions. Particularly,

$$\text{Decreasing filter} = [(-1)^{i+1}, \text{ for } 0 \leq i \leq h - 1], \quad (8)$$

$$\text{Increasing filter} = [(-1)^i, \text{ for } 0 \leq i \leq h - 1], \quad (9)$$

$$\text{Peak filter} = \begin{cases} -\frac{3}{h} \left[ \binom{h-3}{3} C i \right], & \text{for } 0 \leq i \leq \frac{h-3}{3}, \\ \frac{6}{h} \left[ \binom{h-3}{3} C \left( i - \frac{h}{3} \right) \right], & \text{for } \frac{h}{3} \leq i \leq 2 \left( \frac{h-3}{3} \right) + 1, \\ -\frac{3}{h} \left[ \binom{h-3}{3} C \left( i - 2 \left( \frac{h-3}{3} \right) - 2 \right) \right], & \text{for } 2 \left( \frac{h-3}{3} \right) + 2 \leq i \leq h - 1, \end{cases} \quad (10)$$

where  $nCk$  is the binomial coefficient formula. These hand-crafted filters are then utilized within a BC layer (2). The remaining BC layers are learnable, with the number of filters within a given convolution denoted by the numbers in the brackets in Figure 2. In our applications, we found that BC layers with  $z = \{3, 6, 12, 18, 24, 30, 36\}$  work well but alternative filter lengths could be helpful depending on the application, the length of the time series, and temporal resolution, etc. We utilize causal padding (van den Oord et al. [2016]) which does not allow the leakage of future time points into the convolutions applied to the most present time point. We also use dilated convolutions, in which we increase the dilation rate exponentially in each subsequent BC layer which increases the receptive field of the network (Yu and Koltun [2016]), by doubling the dilation rate each time. We also utilize several dense layers wrapped in a concrete dropout layer with the number of nodes in a particular layer given in the brackets in Figure 2. Within the time-distributed dense layer, we subsequently rewrite its output by adding an additional column to represent the variance, where we set the variance of the learned abstract representation of the series to zero, since the time series is observed, and then combine this with the forecast mean and variance from the Welford mean-variance layer in the concatenation layer (Section 2.2). For the activation functions in our network, we use the rectified linear unit function (ReLU) and leaky ReLU function with a slope of 0.01.

The intuition for the network is that the hand-crafted filters (increasing, decreasing, and peak filters), although designed for classification, represent key components of time series in general and would prove useful for the forecasting task, too. Therefore, the learnable representations from the forecasting task should also be able to help with the classification task, and we can feed the learned representation of the observed time series from the forecasting task, in combination with the forecast mean and variance, into the classification component (blue nodes) of the network.

## 4 Simulation results

We perform several simulations to compare our model with current state-of-the-art methods in the time series classification literature. Specifically, we compare our network, which we will call ForeClassNet, with Multi-Rocket HYDRA, an inception network, Hive-Cote 2, and TEASER. The simulations consist of standard time series classification tasks, particularly distinguishing observations from different stochastic processes such as an autoregressive process or a moving average process. We also test the robustness of our method in several adversarial scenarios such as data mislabeling or using the fast gradient sign method (Goodfellow et al. [2015]) with respect to the categorical cross-entropy loss function and the mean squared error loss function.

In our simulations, we compute two measures to compare ForeClassNet and the competing methods. We first record the test set accuracy, on a scale from 0 to 1 with 1 corresponding to perfect accuracy, the proportion of examples in the test set that a given model correctly classifies. We also consider the F1 score, which is the harmonic mean of precision and recall. Specifically, the F1 score =  $\frac{2TP}{2TP+FP+FN}$ , where TP represents the number of true positives, FP represents the number of false positives and FN represents the number of false negatives. The F1 score is also measured on a scale from 0 to 1 where 1 indicates perfect precision and recall. For all of our examples, we utilize the Python programming language (Van Rossum and Drake [2009]). For implementing our network, we use Tensor flow (Abadi et al. [2015])

and <https://github.com/aurelio-amerio/ConcreteDropout>. For implementing the competing methods we use the `aeon` package (Middlehurst et al. [2024a]) for Multi-Rocket Hydra (MR-Hydra), TEASER, and HIVECOTE 2 (HC2) and `sktime` for the inception classifier. We train our model using the ADAM optimization algorithm (Kingma and Ba [2015]) for 100 epochs with a batch size of 64, utilize a train-test split of 80% – 20% reserving 10% of the training data as a validation set.

Notebooks containing the results discussed and the code to produce those results can be found here: <https://danielcoulson.github.io/research/>

#### 4.1 Autoregressive or moving average process

We consider simulating time series from an autoregressive process and a moving average process and then train models to classify which of the processes produced the realized time series. Specifically, we consider the following two processes:

$$X_t = 0.6X_{t-1} - 0.3X_{t-2} + 0.2X_{t-3} + \epsilon_t, \epsilon_t \sim N(0, 1) \text{ iid}, \quad (11)$$

$$\text{and } Y_t = 0.5\eta_{t-1} + 0.4\eta_{t-2} + \eta_t, \eta_t \sim N(0, 1) \text{ iid}. \quad (12)$$

We simulate 10,000 time series each of length 50, where each time series is generated from either process (11) or process (12) with 0.5 probability. To create the forecasting problem, we set the first 40 points as observed points in the time series and the remaining 10 points as future unobserved time points. To compare our method with the state-of-the-art methods from the time series classification literature, we train separate models on the observed and combination of the observed and future time series which we call the full time series. We train the neural network approaches for 100 epochs each without further data pre-processing or hyper parameter tuning. The results can be seen in Table 1.

All models perform reasonably well with the deep learning approaches (ForeClassNet and Inception) achieving superior performance compared to the non-deep learning

Model	accuracy *	F1 *	accuracy	F1
ForeClassNet	1.00	1.00	NA	NA
TEASER	0.86	0.86	NA	NA
Inception	0.98	0.98	0.99	0.99
MR-Hydra	0.88	0.88	0.91	0.91
HC2	0.94	0.94	0.96	0.96

Table 1: Results comparing five time series classification methods on their ability to distinguish between process (11) and process (12). Columns with an asterisk denote the results for models trained on only the observed time series. Columns without an asterisk denote models which are trained on the full time series.

approaches (TEASER, MR-Hydra and HC2). Similarly, all models achieve high F1 scores, with the deep learning approaches scoring highest. However, in general ForeClassNet achieves superior performance in both metrics.

## 4.2 Distinguishing between two Autoregressive processes

Now we switch to the scenario in which we want to distinguish between two different autoregressive processes, which is a more challenging scenario compared to Section 4.1. We consider the following two stochastic processes:

$$X_t = 0.6X_{t-1} - 0.3X_{t-2} + 0.2X_{t-3} + \epsilon_t, \epsilon_t \sim N(0, 1)iid, \quad (13)$$

$$\text{and } Y_t = 0.7Y_{t-1} - 0.4Y_{t-2} + \eta_t, \eta_t \sim N(0, 1)iid. \quad (14)$$

We simulate 10,000 time series each of length 50 where each time series is generated from either (13) or (14) with 0.5 probability. For the forecasting problem, we set the first 40 time points as observed points in the time series and the remaining 10 points as future unobserved time points. The results of each of the models are shown in Table 2. In Table 2 many of the methods see noticeable decreases in accuracy compared to Section 4.1. However, our ForeClassNet maintains its high test set accuracy. The second-best performing model is the inception network which sees a test set accuracy nine percentage points smaller than that of ForeClassNet. However, inception receives a boost in test set accuracy when trained on the full time series, rather than just the

Model	accuracy *	F1 *	accuracy	F1
ForeClassNet	1.00	1.00	NA	NA
TEASER	0.75	0.75	NA	NA
Inception	0.91	0.91	0.97	0.97
MR-Hydra	0.78	0.78	0.81	0.81
HC2	0.88	0.88	0.89	0.89

Table 2: Results comparing five time series classification methods in their ability to distinguish between two autoregressive processes. Columns with an asterisk denote the results for models trained on only the observed time series. Columns without an asterisk denote models which are trained on the full time series.

Model	accuracy *	F1 *	accuracy	F1
ForeClassNet	0.81	0.81	NA	NA
TEASER	0.64	0.64	NA	NA
Inception	0.79	0.79	0.82	0.82
MR-Hydra	0.68	0.68	0.70	0.70
HC2	0.84	0.84	0.83	0.83

Table 3: Results comparing five time series classification methods in distinguishing between two autoregressive processes under data mislabeling. Columns with an asterisk denote the results for models trained on only the observed time series. Columns without an asterisk denote models which are trained on the full time series.

observed time series. But this boost still does not achieve the same test set accuracy as ForeClassNet. The non-deep learning models (HC2, MR-Hydra, and TEASER) do not see a boost in their accuracy scores when trained in the full time series.

### 4.3 Distinguishing between two autoregressive processes subject to severe training data mislabeling

This simulation scenario is the same as that of Section 4.2 but we corrupt the training data by randomly switching the label of 20% of the training data. We then evaluate each of the models on uncorrupted test set data. The results are displayed in Table 3. All models see a decrease in their training set accuracy with ForeClassNet still competitive with respect to the other methods, but HC2 achieves a slightly superior test set accuracy.

Model	accuracy *	Macro F1 *	Weighted F1 *	accuracy	Macro F1	Weighted F1
ForeClassNet	0.92	0.93	0.92	NA	NA	NA
TEASER	0.46	0.46	0.46	NA	NA	NA
Inception	0.88	0.88	0.88	0.91	0.91	0.91
MR-Hydra	0.77	0.77	0.77	0.82	0.81	0.82
HC2	0.91	0.91	0.91	0.93	0.93	0.93

Table 4: Results comparing five time series classification methods under inclusion of a third class. Columns with an asterisk denote the results for models trained on only the observed time series. Columns without an asterisk denote models which are trained on the full time series.

#### 4.4 Distinguishing between two autoregressive processes and their linear combination

In this section we build upon the simulation scenario of Section 4.2 but now introduce a third class which is a linear combination of processes (13) and (14), that is  $0.6 \times$  process (13) +  $0.4 \times$  process(14). A realization of a time series is generated from one of these three classes each with an equal probability of  $\frac{1}{3}$ . The results are displayed in Table 4. All methods see a degradation in performance on the test set with respect to accuracy, and averaged F1 scores compared to Table 2. ForeClassNet still achieves the greatest performance in terms of test set accuracy along with HC2 with all the other methods seeing a slight boost in test set performance when they have access to the full time series.

#### 4.5 Distinguishing two autoregressive processes with adversarial training with respect to the categorical cross entropy loss function

This is a simulation scenario similar to that in Section 4.2 but now we use the fast gradient sign method applied to the categorical cross entropy loss function, that is, we alter the input time series to maximize the loss of the ForeClasNet model with respect to the categorical cross entropy loss. We only adversarially manipulate the input to hinder ForeClassNet we do not perform any manipulation of the input with respect to the other models, and they are simply trained and evaluated on the same training and



test data as ForeClassNet. We train ForeClassNet with the original training data and evaluate it on an adversarial test set. Then we reinitialize the model and train it on a combination of the original training data and adversarial training data, and assess its performance on the original and a new adversarially perturbed test set.

In Sections 4.5 and 4.6, we use the fast gradient sign method to construct adversarial data. This method takes a trained model and computes the derivatives of the loss function with respect to a given input into the network. The adversarial example is then constructed by adding some scalar multiple of the sign of the derivative of the loss to the original input. The multiple of the sign of the gradient of the loss you add to the original input is a term to be specified by the user, where we set the multiplier to be 0.1. In particular,  $x_{\text{adversarial}} = x + 0.1 \text{sign}(\nabla_x L(\cdot))$ , where in our case  $x$  is a single observation of a given time series, and  $L(\cdot)$  is the loss function of interest.

The results of the absence of adversarial training and the evaluation of ForeClassNet on its own adversarial test set (test set a), where the other models are trained on the observed series rather than the entire series, are shown in Table 5. We can see that ForeClassNet takes a severe dip (51 percentage points) in test set performance compared to Table 2, which is expected since we have constructed a test set to maximize the loss of ForeClassNet without performing any adversarial training before evaluating ForeClassNet on the test set. Some of the methods such as TEASER, and MR-Hydra do not see a noticeable reduction in test set performance, which is expected as the test set was constructed to only maximize the loss of ForeClassNet so other models should be affected minimally. Interestingly, some of the other models also see a moderate to severe drop in test set performance. HC2 sees a 13-percentage point decrease in test set accuracy, and Inception sees a 43-percentage point decrease in performance. This could reflect that some of the components of these models reflect similar representations or focus on similar sections of the time series. This harks back to the discussion in the Introduction with respect to hand-crafted filters. That is, there are some fundamental aspects of time series that humans will look at when performing different tasks with

Model	Accuracy(a)	F1(a)
ForeClassNet	0.49	0.33
TEASER	0.70	0.70
Inception	0.48	0.35
MR-Hydra	0.77	0.77
HC2	0.75	0.75

Table 5: Results comparing five time series classification methods under adversarial test set construction with respect to the categorical cross entropy loss function for ForeClassNet when evaluated on test set (a).

Model	Accuracy (b)	F1 (b)	Accuracy (a)	F1 (a)	Accuracy (c)	F1 (c)
ForeClassNet	0.99	0.99	0.99	0.99	0.50	0.35
TEASER	0.74	0.74	0.71	0.71	0.72	0.72
Inception	0.91	0.91	0.91	0.91	0.61	0.57
MR-Hydra	0.76	0.76	0.75	0.75	0.70	0.70
HC2	0.86	0.86	0.82	0.82	0.79	0.79

Table 6: Results comparing five time series classification methods under adversarial test set construction with respect to the categorical cross entropy loss function for ForeClassNet when evaluated on test sets (a-c).

time series, and we see that some very different models may also be focusing on similar fundamental aspects of time series.

We now repeat this, but train the model on the original training data and adversarial training data. The results are displayed in Table 6, where we evaluate this trained model on its own newly constructed adversarial test (c). Through adversarial training, we see that the test set accuracy of ForeClassNet on test sets (a) and (b) increases by 50 percent points, comparable to the results in Table 2. However, there is a lack of improvement in performance in new adversarial attacks when comparing the accuracy of test set (c) to the accuracy of test set (a) in Table 5. MR-Hydra and TEASER maintain a comparable performance to the results in Table 5, and the Inception network sees a slight boost in accuracy in test set (c) compared to Table 5, but is still 30-percentage point less than its test set (b) and (a) accuracy. Overall ForeClassNet maintains superior performance in test set accuracy on its training data despite adversarial attack with respect to the categorical cross entropy loss function, but suffers from under performance in newly constructed adversarial test sets.

Model	accuracy (a)	F1 (a)
ForeClassNet	0.48	0.32
TEASER	0.75	0.75
Inception	0.61	0.56
MR-Hydra	0.79	0.79
HC2	0.84	0.84

Table 7: Results comparing five time series classification methods under adversarial test set construction with respect to the mean squared error loss function for ForeClassNet evaluated on test set (a).

#### 4.6 Distinguishing two autoregressive process with adversarial training with respect to the mean squared error loss function

In this section we repeat the process of Section 4.5 but apply the fast gradient sign method with respect to the mean squared error loss function. We first train ForeClassNet on the original training data and then construct an adversarial test set using the fast gradient sign method (a). The results are displayed in Table 7. We see that some of the other methods maintain their test set performance in the adversarial test set compared to their performance on the original test given in Table 2, particularly TEASER and MR-Hydra. ForeClassNet sees a 52 percent point decrease in the performance of the test set compared to Table 2, which is expected, as we have constructed a test set to maximize the loss without any additional training. Similarly to Section 4.5 we see that Inception sees a 30-percentage point decrease in its test set accuracy and HC2 a 4-percentage point decrease in test set accuracy when compared to their results on the original test set (see Table 2).

We now re-initialize ForeClassNet and train it on both original and adversarial training data and evaluate it on its own newly created adversarial test set (c) and the original test set (b). The results are displayed in Table 8. ForeClassNet achieves comparable performance on the test set (b) compared to Table 2, and achieves superior accuracy on the test set (c) compared to competing methods. Inception sees a boost in its test set accuracy compared to Table 7, with the other methods achieving similar results to those of Table 7. This example demonstrates the robustness of ForeClassNet

Model	accuracy (b)	F1 (b)	accuracy (a)	F1 (a)	Accuracy (c)	F1 (c)
ForeClassNet	0.97	0.97	0.95	0.95	0.94	0.94
TEASER	0.74	0.74	0.76	0.76	0.75	0.75
Inception	0.92	0.91	0.91	0.91	0.92	0.92
MR-Hydra	0.79	0.79	0.78	0.78	0.78	0.78
HC2	0.86	0.86	0.86	0.86	0.86	0.86

Table 8: Results comparing five time series classification methods under adversarial test set construction with respect to the mean squared error loss function for ForeClassNet evaluated on test sets (a-c).

to adversarial attacks with respect to the forecasting component of the problem.

## 5 Real world data results

In this section, we present the application of our model to two real-world data sets. Firstly, we apply our model to the ECG5000 data set to compare the classification performance of ForeClassNet with the state-of-the-art classification methods, which are designed purely for classification rather than forecasting and classification. This also allows us to assess the performance of our model with a relatively small number of training examples for deep learning models, with our model having over 1.3 million trainable parameters. We then apply our model to historical US stock prices and earnings data, which can be found here: <https://www.kaggle.com/datasets/tsaustin/us-historical-stock-prices-with-earnings-data/data> which highlights the unique capabilities of ForeClassNet.

Notebooks containing the results discussed and the code to produce those results may be found here: <https://danielcoulson.github.io/research/>

### 5.1 ECG data

In this section we apply our model to the ECG 5000 data set (Goldberger et al. [2000] and Chen et al. [2015]). There are five classes in this data set that represent five different heart conditions. The classes are Normal, R-on-T premature ventricular contraction,

Model	accuracy *	macro F1 *	weighted F1	accuracy	macro F1	weighted F1
ForeClassNet	0.96	0.62	0.95	NA	NA	NA
TEASER	0.96	0.61	0.95	NA	NA	NA
Inception	0.96	0.64	0.95	0.95	0.63	0.95
MR-Hydra	0.96	0.64	0.95	0.96	0.72	0.96
HC2	0.96	0.64	0.96	0.96	0.64	0.96

Table 9: Results comparing five time series classification methods for the ECG 5000 classification problem. Columns with an asterisk denote the results for models trained on only the observed time series. Columns without an asterisk denote models which are trained on the full time series.

Supraventricular Premature or Ectopic beat, Premature ventricular contraction, and Unclassifiable Beat. This data set consists of only 5000 observed time series, and is a highly unbalanced problem, which is expected as most people will not have heart conditions. In particular, there are 2919 occurrences of the first class, 1767 occurrences of the second class, 194 occurrences of the third class, 96 occurrences of the fourth class, and 24 occurrences of the fifth class. We perform a train-test split where we save 80% of the data for training and the remaining 20% for testing. In ForeClassNet training, we reserve another 10% of the training set as a validation set. We train with a batch size of 64 for 100 epochs using the ADAM stochastic optimization algorithm. To create the forecasting problem, we remove the last five time points from each time series to create the observed time series and train ForeClassNet and TEASER on this alternative problem. We train the standard time series classification methods we compare ForeClassNet to both on only the observed and then the full time series. The results rounded to two decimal places are displayed in Table 9. We see that ForeClassNet achieves the same performance as the state-of-the-art methods on this problem, including when the standard time series classification methods have access to the full time series.

Unfortunately, the F1 scores of all the methods are undesirably low, which results from the unbalanced nature of the data set and also prevents the models from achieving greater generalization performance. This is undesirable from a medical diagnosis perspective as we are concerned with diagnosing patients who suffer from the less obvious

Model	accuracy *	macro F1 *	weighted F1	accuracy	macro F1	weighted F1
ForeClassNet	0.99	0.99	0.99	NA	NA	NA
TEASER	0.99	0.99	0.99	NA	NA	NA
Inception	1.00	1.00	1.00	1.00	1.00	1.00
MR-Hydra	0.99	0.99	0.99	1.00	1.00	1.00
HC2	1.00	1.00	1.00	0.99	0.99	0.99

Table 10: Results comparing five time series classification methods for the ECG 5000 classification problem. Columns with an asterisk denote the results for models trained on only the observed time series. Columns without an asterisk denote models which are trained on the full time series.

conditions. To alleviate this, we utilize the Synthetic Minority Oversampling Technique (SMOTE) proposed in Chawla et al. [2002]. This technique generates new synthetic examples from the minority classes by finding some number of nearest neighbors to a randomly chosen example from the minority class. A neighbor is then chosen randomly, and a synthetic example is generated from the line segment connecting the two examples in feature space. Note that there are other techniques like SMOTE designed explicitly for time series, however, as SMOTE gives us practically perfect performance, and the focus of this paper is not unbalanced data we do not explore these methods further. In particular, we apply SMOTE to the data set, so our modified data set includes 2919 examples of each class. We then repeat the training procedure described above (but train deep learning approaches for 200 rather than 100 epochs), and the associated results are displayed in Table 10. By using SMOTE we increase the performance of all the models to near perfect test set accuracy and F1 score with ForeClassNet achieving similar test set performance to the competing methods. We also propose to use Saliency plots (Simonyan et al. [2014]) from the computer vision literature to provide additional explainability for our proposed model. This explainability would be helpful for sensitive applications of time series classification, such as medical diagnosis. Saliency plots provide us with a way to show which aspects of the input the model is focusing on, specifically which aspects of the input would lead to the largest change in the output if we changed the input value. We provide saliency plots for ForeClassNet in Figures 3-7, which informs the medical practitioner of which parts of the input time series the

model is focusing on. This provides greater explainability to what might otherwise be seen as a black-box model and allows the practitioner to answer meaningful questions from the patient such as "Why have you diagnosed me with this heart condition?" It also allows the practitioner to use their own judgment with respect to medical diagnosis in the cases where the model could give an incorrect output using the saliency plots as a starting point for their own analysis.

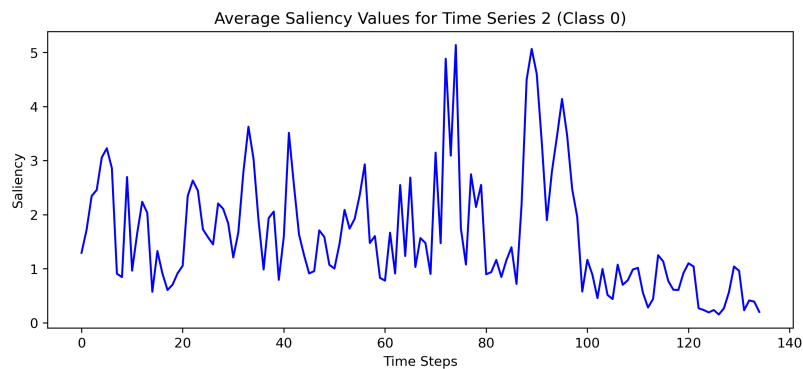


Figure 3: Saliency plot for the second time series in the test set which was in class 0 .

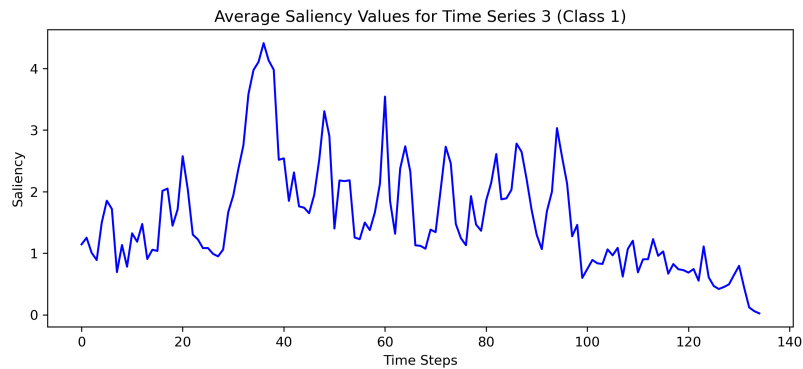


Figure 4: Saliency plot for the third time series in the test set which was in class 1 .

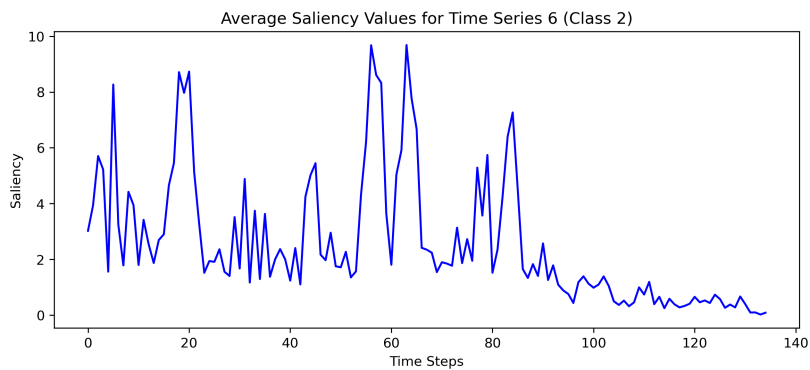


Figure 5: Saliency plot for the sixth time series in the test set which was in class 2 .

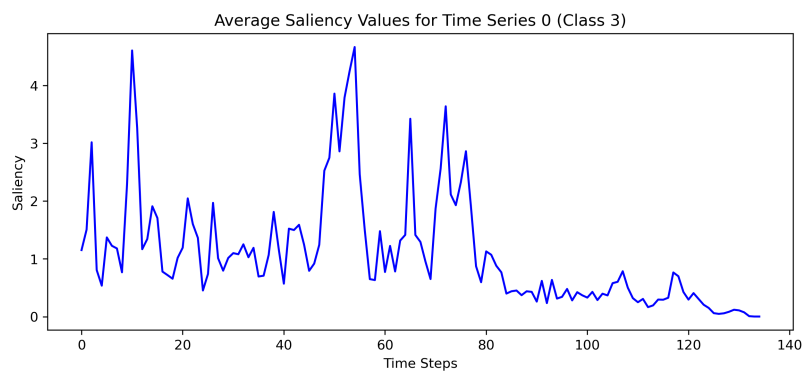


Figure 6: Saliency plot for time series zero in the test set which was in class 3 .

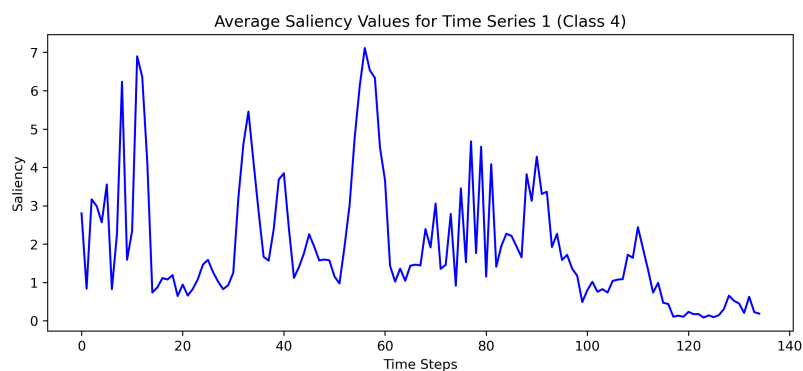


Figure 7: Saliency plot for the first time series in the test set which was in class 4 .

## 5.2 Stock price data

In this section we address the following problem which is of interest to traders in the financial markets. Particularly, based on the 40 previous daily adjusted closing prices



of a given stock, will a company's adjusted closing price increase by 5% or more the day after the release of its quarterly earnings. To answer this question, we use the US historical stock prices with earnings data set from Kaggle. This data set consists of 7786 unique stocks, with the dates of the release of their earnings, whether the release was before or after the market opens, and the daily adjusted closing prices. We firstly extract the time series which have at least 40 days of adjusted closing prices prior to the release of the company's quarterly earnings, we also extract the adjusted closing price of the stock that immediately follows the earnings release. For each time series we then assign it to class one if the price increases by 5% or more after the release of the companies earnings compared to the previous adjusted closing price, and class zero otherwise. This results in 90,000 time series consisting of 40 daily adjusted closing prices before the release of a company's earnings, the adjusted closing price after the release of the company's earnings, and the class label for each time series. This is a fairly balanced problem, and we do not use any data augmentation techniques such as SMOTE to increase the representation of time series belonging to a particular class. We assign 80,000 time series to the training set, and 10,000 of the time series to the test set; we further set aside 10% of the training data for a validation set. We train ForeClassNet using the Adam optimization algorithm, with a MSE loss function for the forecasting component of our model and the categorical cross entropy loss function for the classification component of our model. We train ForeClassNet for 100 epochs with a batch size of 128. Similarly, we train inception for 100 epochs with a batch size of 128. Due to the difficulty of this problem and the relatively large training set size we utilize early stopping for the training of ForeClassNet with a patience of 10 epochs. The implementation of the inception network does not allow monitoring of a validation set natively, so we instead fit multiple inception networks trained for an increasing number of epochs and choose the one which achieves the highest accuracy on the validation set. Unfortunately, the other models cannot seem to handle the large size of this problem which resulted in the crashing of the python session we were using,

Model	accuracy *	F1 *	accuracy	F1
ForeClassNet	0.75	0.75	0.73	0.73
TEASER	NA	NA	0.53	0.52
Inception	0.51	0.34	0.51	0.34
MR-Hydra	NA	NA	0.55	0.55
HC2	NA	NA	0.58	0.58

Table 11: Results comparing five time series classification methods for stock price prediction focused around the release of companies quarterly earnings. Columns with an asterisk denote model trained on all 80,000 time series, columns without an asterisk denote columns trained on the subset of the data consisting of 10,000 time series. Models trained on the full data set and the subset of the data set were evaluated on the same test set.

therefore to allow some comparison we train the remaining methods on a subset of the training data consisting of only 10,000 time series with 5000 time series belonging to each class. ForeClassNet provides a classification decision based on what it has seen in the past time series, and what it thinks it will see in the future and its associated uncertainty, whereas the other models do not enforce this behavior. To reiterate, when it comes to inference time all methods receive the exact same time series each of length 40, and for a given time series none of the models receive any information as to what the adjusted closing price will be the next day. The results are displayed in Table 11.

As can be seen in Table 11, ForeClassNet achieves vastly superior results compared to competing methods, achieving a 29.3% improvement in test set accuracy over the next-best competing method and a 47% improvement in test set accuracy compared to the Inception network. When we train ForeClassNet on the subset of the data, it still achieves superior results compared to competing methods with a 26% improvement in test set accuracy compared to the second-best model. In some of our experiments, we noticed a slight variation in ForeClassNet results when using the smaller training set with a test set accuracy ranging from high 60%*s* to low 70%*s* due to the use of random subsetting of the original training data.

## 6 Conclusion

In this article, we have proposed a novel problem called ForeClassing and network architecture called ForeClassNet which achieves superior results compared to current state-of-the-art time series classification models in both simulation and real-world scenarios. To construct this network, we proposed two novel neural network layers, Boltzmann convolutions and Welford mean-variance layers, and proved a motivating theorem, the ForeClassing theorem. Boltzmann convolutions provide a novel approach to capture multi-resolution aspects of a sequential input into a network. Welford mean-variance layers provide a novel way for the network to update its uncertainty about what it thinks will happen in the future, which can be subsequently leveraged in deeper parts of the network. To aid in explaining our model, we propose using saliency plots to capture which aspects the trained ForeClassNet is focusing on for a given input. There are several new avenues for future research in this area, such as new approaches to solving the ForeClassing problem, investigating more applications of Boltzmann Convolutions and Welford mean-variance layer, further exploration of adversarial attacks on ForeClassNet such as working with projected gradient descent, and further theoretical analysis of the ForeClassing problem building upon the statement of the ForeClassing problem and the ForeClassing theorem in Section 2.

## References

Martín Abadi, Ashish Agarwal, Paul Barham, Eugene Brevdo, Zhifeng Chen, Craig Citro, Greg S. Corrado, Andy Davis, Jeffrey Dean, Matthieu Devin, Sanjay Ghemawat, Ian Goodfellow, Andrew Harp, Geoffrey Irving, Michael Isard, Yangqing Jia, Rafal Jozefowicz, Lukasz Kaiser, Manjunath Kudlur, Josh Levenberg, Dandelion Mané, Rajat Monga, Sherry Moore, Derek Murray, Chris Olah, Mike Schuster, Jonathon Shlens, Benoit Steiner, Ilya Sutskever, Kunal Talwar, Paul Tucker, Vincent Vanhoucke, Vijay Vasudevan, Fernanda Viégas, Oriol Vinyals, Pete War-

- den, Martin Wattenberg, Martin Wicke, Yuan Yu, and Xiaoqiang Zheng. TensorFlow: Large-scale machine learning on heterogeneous systems, 2015. URL <https://www.tensorflow.org/>. Software available from tensorflow.org.
- Andrés M Alonso, José R Berrendero, Adolfo Hernández, and Ana Justel. Time series clustering based on forecast densities. *Computational Statistics & Data Analysis*, 51(2):762–776, 2006.
- Anastasia Borovykh, Sander Bohte, and Cornelis W Oosterlee. Conditional time series forecasting with convolutional neural networks. *Stat*, 1050:16, 2017.
- Nitesh V Chawla, Kevin W Bowyer, Lawrence O Hall, and W Philip Kegelmeyer. Smote: synthetic minority over-sampling technique. *Journal of Artificial Intelligence Research*, 16:321–357, 2002.
- Yanping Chen, Yuan Hao, Thanawin Rakthanmanon, Jesin Zakaria, Bing Hu, and Eamonn Keogh. A general framework for never-ending learning from time series streams. *Data Mining and Knowledge Discovery*, 29:1622–1664, 2015.
- Yinpeng Chen, Xiyang Dai, Mengchen Liu, Dongdong Chen, Lu Yuan, and Zicheng Liu. Dynamic convolution: Attention over convolution kernels. In *Proceedings of the IEEE/CVF Conference on Computer Vision and Pattern Recognition*, pages 11030–11039, 2020.
- Andreas Damianou and Neil D Lawrence. Deep gaussian processes. In *Artificial Intelligence and Statistics*, pages 207–215. PMLR, 2013.
- Angus Dempster, Daniel F Schmidt, and Geoffrey I Webb. Hydra: Competing convolutional kernels for fast and accurate time series classification. *Data Mining and Knowledge Discovery*, 37(5):1779–1805, 2023.
- Sylvia Fröhwrth-Schnatter and Sylvia Kaufmann. Model-based clustering of multiple time series. *Journal of Business & Economic Statistics*, 26(1):78–89, 2008.

- Yarin Gal and Zoubin Ghahramani. Dropout as a bayesian approximation: Representing model uncertainty in deep learning. In *International Conference on Machine Learning*, pages 1050–1059. PMLR, 2016.
- Yarin Gal, Jiri Hron, and Alex Kendall. Concrete dropout. *Advances in Neural Information Processing Systems*, 30, 2017.
- Ary L Goldberger, Luis AN Amaral, Leon Glass, Jeffrey M Hausdorff, Plamen Ch Ivanov, Roger G Mark, Joseph E Mietus, George B Moody, Chung-Kang Peng, and H Eugene Stanley. Physiobank, physiokit, and physionet: components of a new research resource for complex physiologic signals. *Circulation*, 101(23):e215–e220, 2000.
- Ian J Goodfellow, Jonathon Shlens, and Christian Szegedy. Explaining and harnessing adversarial examples. In *3rd International Conference on Learning Representations, ICLR 2015, San Diego, CA, USA, May 7-9, 2015, Conference Track Proceedings*, 2015.
- Izzeddin Gür, Mehmet Güvercin, and Hakan Ferhatosmanoglu. Scaling forecasting algorithms using clustered modeling. *The VLDB Journal*, 24:51–65, 2015.
- Jie Hu, Li Shen, and Gang Sun. Squeeze-and-excitation networks. In *Proceedings of the IEEE Conference on Computer Vision and Pattern Recognition*, pages 7132–7141, 2018.
- Ali Ismail-Fawaz, Maxime Devanne, Jonathan Weber, and Germain Forestier. Deep learning for time series classification using new hand-crafted convolution filters. In *2022 IEEE International Conference on Big Data (Big Data)*, pages 972–981. IEEE, 2022.
- Hassan Ismail Fawaz, Benjamin Lucas, Germain Forestier, Charlotte Pelletier, Daniel F Schmidt, Jonathan Weber, Geoffrey I Webb, Lhassane Idoumghar, Pierre-Alain

- Muller, and François Petitjean. Inceptiontime: Finding alexnet for time series classification. *Data Mining and Knowledge Discovery*, 34(6):1936–1962, 2020.
- Diederik P. Kingma and Jimmy Ba. Adam: A method for stochastic optimization. In *3rd International Conference on Learning Representations, ICLR 2015, San Diego, CA, USA, May 7-9, 2015, Conference Track Proceedings*, 2015.
- Taiyeong Lee, Yongqiao Xiao, Xiangxiang Meng, and David Duling. Clustering time series based on forecast distributions using kullback-leibler divergence. *International Institute of Forecasters (IIF)*. Web, 2014.
- Shen Liu, Elizabeth Ann Maharaj, and Brett Inder. Polarization of forecast densities: a new approach to time series classification. *Computational Statistics & Data Analysis*, 70:345–361, 2014.
- Matthew Middlehurst, James Large, Michael Flynn, Jason Lines, Aaron Bostrom, and Anthony Bagnall. Hive-cote 2.0: a new meta ensemble for time series classification. *Machine Learning*, 110(11):3211–3243, 2021.
- Matthew Middlehurst, Ali Ismail-Fawaz, Antoine Guillaume, Christopher Holder, David Guijo-Rubio, Guzál Bulatova, Leonidas Tsaprounis, Lukasz Mentel, Martin Walter, Patrick Schäfer, and Anthony Bagnall. aeon: a python toolkit for learning from time series. *Journal of Machine Learning Research*, 25(289):1–10, 2024a. URL <http://jmlr.org/papers/v25/23-1444.html>.
- Matthew Middlehurst, Patrick Schäfer, and Anthony Bagnall. Bake off redux: a review and experimental evaluation of recent time series classification algorithms. *Data Mining and Knowledge Discovery*, pages 1–74, 2024b.
- Navid Mohammadi Foumani, Lynn Miller, Chang Wei Tan, Geoffrey I Webb, Germain Forestier, and Mahsa Salehi. Deep learning for time series classification and extrinsic regression: A current survey. *ACM Computing Surveys*, 56(9):1–45, 2024.

- Alejandro Pasos Ruiz, Michael Flynn, James Large, Matthew Middlehurst, and Anthony Bagnall. The great multivariate time series classification bake off: a review and experimental evaluation of recent algorithmic advances. *Data Mining and Knowledge Discovery*, 35(2):401–449, 2021.
- Patrick Schäfer and Ulf Leser. Teaser: early and accurate time series classification. *Data Mining and Knowledge Discovery*, 34(5):1336–1362, 2020.
- Karen Simonyan, Andrea Vedaldi, and Andrew Zisserman. Deep inside convolutional networks: Visualising image classification models and saliency maps. In *Proceedings of the International Conference on Learning Representations (ICLR)*. ICLR, 2014.
- Christian Szegedy, Wei Liu, Yangqing Jia, Pierre Sermanet, Scott Reed, Dragomir Anguelov, Dumitru Erhan, Vincent Vanhoucke, and Andrew Rabinovich. Going deeper with convolutions. In *Proceedings of the IEEE Conference on Computer Vision and Pattern Recognition*, pages 1–9, 2015.
- Aäron van den Oord, Sander Dieleman, Heiga Zen, Karen Simonyan, Oriol Vinyals, Alex Graves, Nal Kalchbrenner, Andrew Senior, and Koray Kavukcuoglu. Wavenet: A generative model for raw audio. In *9th ISCA Workshop on Speech Synthesis Workshop (SSW 9)*, page 125, 2016.
- Guido Van Rossum and Fred L. Drake. *Python 3 Reference Manual*. CreateSpace, Scotts Valley, CA, 2009. ISBN 1441412697.
- José A Vilar and Juan M Vilar. Time series clustering based on nonparametric multi-dimensional forecast densities. *Electronic Journal of Statistics*, 7:1019–1046, 2013.
- Tian Wang, Zhaoying Liu, Ting Zhang, and Yujian Li. Time series classification based on multi-scale dynamic convolutional features and distance features. In *2021 2nd Asia Symposium on Signal Processing (ASSP)*, pages 239–246. IEEE, 2021.
- Barry Payne Welford. Note on a method for calculating corrected sums of squares and products. *Technometrics*, 4(3):419–420, 1962.

Fisher Yu and Vladlen Koltun. Multi-scale context aggregation by dilated convolutions.  
In *4th International Conference on Learning Representations, ICLR 2016, San Juan, Puerto Rico, May 2-4, 2016, Conference Track Proceedings*, 2016.